Ex Vivo–Induced Bone Marrow-Derived Myeloid Suppressor Cells Prevent Corneal Allograft Rejection in Mice

Jun Zhu,[1–3] Takenori Inomata,[1,3,4–6] Keiichi Fujimoto,[1] Koichiro Uchida,[7] Kenta Fujio,[1,6] Ken Nagino,[5] Maria Miura,[1,6] Naoko Negishi,[7,8] Yuichi Okumura,[1,4,6] Yasutsugu Akasaki,[1,6] Kunihiko Hirosawa,[1,6] Mizu Kuwahara,[1,6] Atsuko Eguchi,[5] Hurramhon Shokirova,[1] Ai Yanagawa,[6] Akie Midorikawa-Inomata,[5] and Akira Murakami[1,3,5]

[1]Department of Ophthalmology, Juntendo University Graduate School of Medicine, Tokyo, Japan
[2]Department of Ophthalmology, Subei People's Hospital Affiliated to Yangzhou University, Jiangsu Province, China
[3]Department of Ophthalmology, Juntendo University Faculty of Medicine, Tokyo, Japan
[4]Department of Strategic Operating Room Management and Improvement, Juntendo University Graduate School of Medicine, Tokyo, Japan
[5]Department of Hospital Administration, Juntendo University Graduate School of Medicine, Tokyo, Japan
[6]Department of Digital Medicine, Juntendo University Graduate School of Medicine, Tokyo, Japan
[7]Atopy Research Center, Juntendo University Graduate School of Medicine, Tokyo, Japan
[8]Department of Indoor Environment Neurophysiology Research, Juntendo University Graduate School of Medicine, Tokyo, Japan

Correspondence: Takenori Inomata, Juntendo University Graduate School of Medicine, Department of Ophthalmology, 3-1-3 Hongo, Bunkyo-ku, Tokyo 113-0033, Japan; tinoma@juntendo.ac.jp.

Received: November 14, 2020
Accepted: May 2, 2021
Published: June 1, 2021

Citation: Zhu J, Inomata T, Fujimoto K, et al. Ex vivo–induced bone marrow-derived myeloid suppressor cells prevent corneal allograft rejection in mice. *Invest Ophthalmol Vis Sci.* 2021;62(7):3. https://doi.org/10.1167/iovs.62.7.3

Purpose. To investigate the effects of ex vivo–induced bone marrow myeloid-derived suppressor cells (BM-MDSCs) on allogeneic immune responses in corneal transplantation.

Methods. Bone marrow cells from C57BL/6J (B6) mice were cultured with IL-6 and GM-CSF for four days. The ex vivo induction of the BM-MDSCs was assessed using flow cytometry, inducible nitric oxide synthase (iNOS) mRNA expression using reverse transcription–quantitative polymerase chain reaction, and nitric oxide (NO) production in allogeneic stimulation. T-cell proliferation and regulatory T-cell (Treg) expansion were investigated on allogeneic stimulation in the presence of ex vivo–induced BM-MDSCs. IFN-γ, IL-2, IL-10, and TGF-β1 protein levels were measured using enzyme-linked immunosorbent assays. After subconjunctival injection of ex vivo–induced BM-MDSCs, the migration of the BM-MDSCs into corneal grafts, allogeneic corneal graft survival, neovascularization, and lymphangiogenesis were assessed using flow cytometry, slit-lamp microscopy, and immunohistochemistry.

Results. The combination of GM-CSF and IL-6 significantly induced BM-MDSCs with increased *iNos* mRNA expression. The ex vivo–induced BM-MDSCs promoted NO release in allogeneic stimulation in vitro. The ex vivo–induced BM-MDSCs inhibited T-cell proliferation and promoted Treg expansion. Decreased IFN-γ and increased IL-2, IL-10, and TGF-β1 production was observed in coculture of ex vivo–induced BM-MDSCs. Injected ex vivo–induced BM-MDSCs were confirmed to migrate into the grafts. The injected BM-MDSCs also prolonged corneal graft survival and prevented angiogenesis and lymphangiogenesis.

Conclusions. The ex vivo–induced BM-MDSCs have suppressive effects on allogeneic immune responses and prolong corneal allograft survival via the iNOS pathway, indicating that they may be a potential therapeutic tool for corneal transplantation.

Keywords: MDSC, corneal transplantation, immune privilege, regulatory T cell, allograft rejection

Corneal transplantation is the most common tissue transplantation worldwide[1,2] and is associated with high success rates owing to its immune privilege.[3] However, high-risk corneal transplantation characterized by angiogenesis and inflammation caused by infection, autoimmune disease, or re-transplantation results in graft rejection in 41% to 100% of cases.[4–6] Treatment with immunosuppressive agents, such as steroids, cyclosporine, and tacrolimus, has significantly reduced the rate of acute rejection after corneal transplantation. However, this therapeutic advance remains associated with several problems, including reduced therapeutic effectiveness on chronic rejection and undesirable side

effects, such as cataract, glaucoma, diabetes, and opportunistic infections. Therefore it is clinically important to ensure long-term immune tolerance for the maintenance of the transplanted organ.

During the corneal allograft rejection process, the newly formed vasculature introduces allogeneic antigens from the donor into the cervical draining lymph nodes where the recipient's immune system deems them foreign invaders. This process activates host T cells to target the graft, ultimately leading to tissue damage. Regulatory T cells (Tregs) have an antigen-specific suppressive function in the immune response to corneal transplantation.[7,8] However, the expansion of the Treg population requires activation of the transcription factor forkhead box P3 (Foxp3) and the formation of a Treg-type epigenome, which are triggered via T-cell receptor stimulation.[9] Additionally, the plasticity of Tregs, in which Foxp3 expression is reduced in an inflammatory environment, has become apparent.[10,11] Therefore it has been difficult to expand Tregs in human organisms.[12] To overcome this limitation, it is important to find ways to effectively promote Treg expansion, as well as to elucidate the immunosuppressive pathways involved in Treg induction in the inflammatory environment. Such knowledge is critical to achieve better corneal transplantation outcomes.

Myeloid-derived suppressor cells (MDSCs) are progenitors of granulocytic cells and are induced under pathological conditions, such as cancer and in conditions associated with chronic inflammation. Different cell therapies, including ex vivo-generated dendritic cells, mesenchymal stromal cells, and ex vivo–induced Tregs, have been investigated, and exhibited promising prospects.[13-15] In mice, MDSCs express the myeloid lineage marker CD11b and the granulocytic marker Gr1 on their surface.[16] Importantly, MDSCs can induce Tregs and inhibit effector T cell proliferation,[17] although the underlying process remains unclear. Notably, MDSCs can be induced in vitro by culturing bone marrow cells in the presence of signaling factors from the microenvironment of cancer and inflammatory diseases.[18] In mice corneal transplantation, MDSCs prompted effective results. For example, Ren et al.[19] reported that these cell improved graft survival through suppressing angiogenesis and lymphangiogenesis. Therefore the application of ex vivo–induced bone marrow MDSCs (BM-MDSCs) is promising for high-risk corneal transplantation in a local inflammatory environment as a potential approach for preventing graft rejection.

Thus this study aimed to investigate the immunosuppressive effect of ex vivo–induced BM-MDSCs in an inflamed corneal environment using a high-risk corneal transplantation mouse model.

Methods

Animals and Anesthesia

Six- to eight-week-old BALB/c (H-2d), C57BL/6 (H-2b), and CBA/J male mice were purchased from Sankyo Labo Service Corporation (Tokyo, Japan). Foxp3^{hCD2} reporter mice (BALB/c) were kindly supplied by Dr. Shohei Hori from the Laboratory of Immunology and Microbiology, University of Tokyo. B6 transgenic mice expressing enhanced GFP were raised at the Atopy Research Center, Juntendo University Graduate School of Medicine, Tokyo, Japan, and housed under pathogen-free conditions. The corneal transplantation procedure was performed under intraperitoneal administration of anesthetics ketamine and xylazine solutions at doses of 120 and 20 mg/kg body weight, respectively. All animal experiments were approved by the Institutional Animal Care and Use Committee of the Juntendo University, Faculty of Medicine (approval no. 310062) and conducted in accordance with the Association for Research in Vision and Ophthalmology Statement for the Use of Animals in Ophthalmic and Vision Research.

BM-MDSC Culture

BM-MDSCs were cultured as previously reported.[20] Briefly, BM was collected from mouse femurs and treated with red blood cell lysis buffer (BioLegend, San Diego, CA, USA). Isolated BM immune cells were then washed with 10% fetal bovine serum (FBS) and filtered through a 40-µm strainer (Greiner Bio-One, Kremsmünster, Austria). Thereafter, 3×10^6 cells were resuspended in 14 mL of culture medium: 500 mL Roswell Park Memorial Institute-1640 media (Lonza, Basel, Switzerland) supplemented with 55 mL FBS (Atlanta Biologicals, Flowery Branch, GA, USA), 2 µL 2-mercaptoethanol, 12.5 mL 1 M HEPES (Thermo Fisher Scientific, Waltham, MA, USA), 500 mg streptomycin sulfate (Meiji Seika, Chuo City, Tokyo Japan), and 5 mL 100 mM sodium pyruvate (Sigma-Aldrich, St. Louis, MO, USA). To generate BM-MDSCs, interleukin (IL)-6 (Peprotech, Rocky Hill, NJ, USA) and granulocyte macrophage-colony stimulating factor (GM-CSF; Peprotech) were added, each at 40 ng/mL. The BM-derived cells were cultured in an incubator at 37°C, 5% CO_2, and 95% humidity for four days for further ex vivo or in vivo studies.

Carboxyfluorescein Diacetate Succinimidyl Ester (CFSE) Labeling

CFSE labeling was performed as described previously.[21] Briefly, 1×10^7 BALB/c mouse lymphocytes isolated from cervical lymph nodes were incubated with 200 µL CFSE (Thermo Fisher Scientific) for five minutes at 37°C. To stop the reaction, the cells were washed twice using the previously described culture medium. Finally, CFSE-labeled cells were counted on a TC20 automated cell counter (Bio-Rad, Hercules, CA, USA) and immediately used for the mixed lymphocyte reaction (MLR) assay.

MLR Assay

CFSE-labeled lymphocytes from BALB/c mice were used as responder cells. For the stimulator cells, B6 mouse splenocytes were cultured and proliferated with lipopolysaccharide for 24 hours and then exposed to gamma-rays (30 Gy). BM-MDSCs from donor B6 mouse were chosen because, in a pilot experiment, we found it to have a stronger effect compared to BALB/c and CBA/J mouse (Supplementary Fig. S2). Before performing the MLR assay, the allogeneic splenocytes were resuspended in the culture medium described above. The responder and stimulator cells were mixed equally at a concentration of 1×10^6 cells/mL. B6 mouse BM-MDSCs were added to the mix and co-cultured at ratios 1:1, 1:3/4, 1:1/2, 1:1/4, 1:1/5, or 1:1/10. The inducible nitric oxide synthase (iNOS) inhibitor N^G-monomethyl-L-arginine (50 µmol/mL) and arginase-1 (ARG1) inhibitor N^{ω}-hydroxy-nor-L-arginine acetate (500 µmol/mL) (475886 and 399275, respectively; MilliporeSigma, Burlington, MA, USA)

were used. The MLR mixtures were cultured in 96-well round-bottom plates. Simultaneously, we evaluated the T-cell response via CD3 stimulation and its expansion using an anti-CD3 antibody (145-2C11, BioLegend). We coated a 24-well plate with 10 µg/mL anti-CD3 antibody in PBS (500 µL/well) and incubated the plate overnight at 4°C. Before use, the wells were washed thrice with sterile PBS to remove unbound soluble antibodies. The responder cells and BM-MDSCs were mixed to a concentration of 1×10^6 cells/mL and incubated for four days at 37°C. Subsequently, lymphocyte proliferation was measured via ^{3}H-thymidine incorporation, that is, the cells were treated with ^{3}H-thymidine (37,000 Bq) 18 hours before the end of the incubation. ^{3}H-thymidine incorporation was measured using the Wallac 1450 MicroBeta Plus counter (PerkinElmer, Waltham, MA, USA).

Griess Nitrite Assay

Supernatant from naive BM cells, or cells treated with IL-6, GM-CSF, or both as well as culture fluid from MLR were taken to measure nitrite concentration using Griess reagent system (Promega, Madison, WI, USA). According to manufacturer's instructions, 50 µL of each sample was added to wells in triplicate. Then, 50 µL of Griess reagent was added into each well and incubated at room temperature for 10 minutes. The absorbance was measured at 540 nm, and nitrite was calculated based on the standard curve.

ELISA

ELISA kits for mouse IFN-γ (DY485), IL-2 (DY402-05), IL-10 (DY417-05), and TGF-β1 (DY1679-05) were purchased (R&D Systems Minneapolis, MN, USA) and used according to the manufacturer's instructions, with the culture supernatants as samples.

Flow Cytometry

BM-MDSCs and grafted cornea were harvested, and single-cell suspensions were prepared as described previously.[22] To avoid nonspecific staining, the cells were treated with an anti-FcR blocking monoclonal antibody (clone 93, no. 14-0161-82; eBioscience, San Diego, CA, USA) and then stained with the respective antibodies: anti-CD11b (M1/70), anti-Gr-1 (RB6-8C5), anti-human CD2 (RPA-2.10), anti-CD4 (GK1.5), and anti-CD8 (53-5.8) antibodies (BioLegend). The stained cells were examined using a BD FACScanto II flow cytometer (BD Bioscience, Franklin Lakes, NJ, USA) and analyzed using FlowJo X 10.0.7 (BD). Additionally, two phenotypes of BM-MDSCs—Ly6G^{low}Ly6C^{hi} and Ly6G^{hi}Ly6C^{low} cells—representing monocytic-MDSCs (MO-MDSCs) and polymorphonuclear MDSCs (PMN-MDSCs), respectively, were sorted using an autoMACS Pro Separator (Miltenyi Biotec, Bergisch Gladbach, Germany).

Corneal Transplantation Protocol

Suture-Induced Inflamed Graft Bed Preparation. Inflamed neovascularized "high-risk" recipient beds were created as detailed previously.[10,23,24] Three intrastromal sutures were placed in the central cornea 14 days before corneal transplantation, using 11–0 sutures (MANI, Tochigi, Japan).

Allogeneic Corneal Transplantation. Murine allogenic corneal transplantation was performed as described previously.[23] Briefly, a central cornea (2-mm diameter) was excised from a donor B6 mouse. The graft bed was prepared by excising a 1.5-mm site in the central cornea of a BALB/c mouse. The donor tissue was then placed onto the recipient bed and secured with eight interrupted 11–0 nylon sutures. After transplantation, the host eyelids were kept closed for three days, and the sutures were removed on day 7. The high-risk corneal transplantation model was established using these high-risk recipient beds.

Grafted Cornea Assessment. Graft's neovascularization score, opacity score, and survival rate were evaluated using a slit-lamp biomicroscope. A standardized scoring system was used to assess the neovascularization score (range, 0–8) and opacity score (range, 0–5+).[23] Corneas with an opacity score of 2+ in two consecutive examinations were considered rejected.

Subconjunctival Injection of Ex Vivo-Induced BM-MDSCs Into Allograft Recipients. The ex vivo–induced BM-MDSCs (1×10^6 cells) were suspended in 10 µL PBS and injected subconjunctivally into allograft recipients using a 33-gauge metal needle and 1-mL syringe (M. S. Surgical, Kalol, India) immediately after corneal transplantation according to previous studies.[19,25,26] The control mice received a PBS injection.

RNA Isolation and RT-qPCR

Total RNA of the ex vivo–induced BM-MDSCs (5×10^6 cells per sample) was isolated using the NucleoSpin RNA isolation kit (Macherey-Nagel, Düren, Germany). cDNA was reverse transcribed from total RNA using random primers and the ReverTra Ace qPCR RT kit (Toyobo, Osaka, Japan) following the manufacturer's guidelines. RT-qPCR was performed using the Applied Biosystems 7500 Fast Real-Time PCR and Life Technology FAST-SYBR Green master mix (Thermo Fisher Scientific). All reactions were performed in triplicate. Results were analyzed using the $2^{-\Delta\Delta Ct}$ method, and *Gapdh* was used as internal control. Specific primer sets were used for *iNos*, *Ifng*, *Tgfb1*, *Il1b*, *Vegfa*, and *Gapdh* in Supplementary Table S1.

Tracking Of Migration Of Subconjunctivally-Injected MDSCs Into Corneal Grafts

The ex vivo–induced BM-MDSCs from GFP-B6 mice were injected subconjunctivally into the transplanted mice 48 hours after corneal transplantation. Then, grafted corneas were harvested, and single-cell suspensions were prepared as described previously.[22]

Immunohistochemistry and Immunofluorescence

The excised corneas were washed with PBS and incubated with anti-FcR CD16/CD32 blocking antibody (clone 93, #14-0161-82; BD Biosciences). After incubation with 20 mM ethylenediamine tetra-acetic acid for 60 minutes at 37°C, the corneal epithelium was removed, fixed in acetone for 15 minutes at 20° to 22°C, and blocked in 2% bovine serum albumin for 60 minutes. The corneas were double-stained overnight for CD31 and lymphatic vessel endothelial hyaluronan receptor-1 (LYVE-1) using goat anti-mouse

FITC-conjugated CD31 (1:100; Santa Cruz Biotechnology, Dallas, TX, USA) and purified goat anti-mouse LYVE-1 (1:400; AF2125, R&D Systems, respectively, as described previously.[5] Cy3-conjugated donkey anti-goat (1:2000, Jackson ImmunoResearch Laboratories, West Grove, PA, USA) antibody was then added as a secondary antibody, followed by incubation for 2 hours. Stained whole corneas were mounted in Vectashield with 4′,6-diamidino-2-phenylindole (Vector Laboratories, Burlingame, CA, USA) and observed under a fluorescence microscope (BZ-X710; Keyence, Osaka, Japan). The area covered by blood or lymphatic vessels of the total cornea was analyzed using ImageJ (National Institutes of Health, Bethesda, MD, USA).[5]

Statistical Analysis

The Mann-Whitney test was used to compare means between groups. Experiments with more than two groups were analyzed using one- or two-way analysis of variance with Bonferroni's multiple comparison post-hoc test. Kaplan-Meier analysis with the log-rank test was used to evaluate graft survival post-corneal transplantation. Data are presented as the means ± SEM and were considered statistically significant at $P < 0.05$. All statistical calculations were performed using Prism 8.0 (GraphPad Software, San Diego, CA, USA).

Results

IL-6 and GM-CSF Promote BM-MDSC Induction, Higher Relative *iNos* Expression, and Increase Nitrite Oxide Release Capability

The $Gr1^+CD11b^+$ double-positive phenotype is recognized as the marker for BM-MDSCs.[27] The mean (± SEM) frequency of $Gr1^+CD11b^+$ BM-MDSCs was 45.4 ± 0.7% in naive BM cells (untreated group), 40.9 ± 1.6% in the IL-6-treated group, 71.9 ± 2.3% in the GM-CSF-treated group, and 75.9 ± 1.7% in the GM-CSF and IL-6-treated group. Compared with the naive BM cell group, the BM-MDSC frequency increased significantly in the combination treatment group (Figs. 1A and 1B; $P < 0.001$). IL-6 treatment alone and GM-CSF and IL-6 co-stimulation increased *iNos* mRNA expression compared with naive BM cells and GM-CSF treated group (Fig. 1C; $P \leq 0.001$). After four days incubation, there were no differences in the measured nitrite levels among the naive BM cell group and the different treatment groups (Fig. 1D). During the MLR assay, nitrite production was significantly increased in the IL-6 and GM-CSF co-treated BM cells compared with the naive BM cells and IL-6 and GM-CSF single treatment groups. The nitrite production in MLR of non-stimulation, allo-stimulation, naive BM cells, and ex vivo–induced BM-MDSC intervention groups were 1.1 ± 0.1 µM, 0.9 ± 0.3 µM, 2.3 ± 0.1 µM, and 28.1 ± 1.0 µM respectively (Fig. 4E; $P < 0.001$). Moreover, GM-CSF and IL-6 costimulus boosted the proliferation of $Ly6G^{low}Ly6C^{hi}$ MO-MDSCs compared with naive BM cells (Figs. 1F and 1G; naive BM cells, 24.3 ± 2.2%; IL-6-treated cells, 23.2 ± 2.7%; GM-CSF-treated cells, 41.4 ± 4.2%; double-treated cells, 46.1 ± 1.8%, $P = 0.001$). However, the frequency of $Ly6G^{hi}Ly6C^{low}$ PMN-MDSCs in the BM-MDSCs decreased (Supplementary Fig. S1; naive BM cells, 57.1 ± 0.7%; IL-6-treated cells, 55.9 ± 1.0%; GM-CSF-treated cells, 37.2 ± 0.8%; double-treated cells, 29.1 ± 0.4%, $P < 0.001$).

Ex Vivo–Induced BM-MDSCs Inhibit T Cell Proliferation

The immunosuppressive effect of ex vivo–induced BM-MDSCs on T cells was assessed using the MLR assay. The ^{3}H-thymidine uptake was evaluated in the T cells cocultured at different ratios with B6 mice naive BM or treated BM cells. No inhibition was observed with naive BM cells (Fig. 2A; naive BM cell/T cell ratio: 1/1, $P > 0.999$; 1/2, $P = 0.109$), and IL-6 (Fig. 2B; IL-6 treated BM cell to T cell ratio: 1/1, $P = 0.653$; 1/2, $P > 0.999$) and GM-CSF treatments (Fig. 2C; GM-CSF-treated BM cell to T cell ratio: 1/1, $P > 0.999$; 1/2, $P = 0.003$). Whereas B6 mice ex vivo–induced BM-MDSCs (GM-CSF plus IL-6 stimulation) significantly inhibited cell proliferation (Fig. 2D; BM-MDSC to T cell ratio: 1/1, $P = 0.005$; 1/2, $P = 0.007$). The experiment-wise comparison among these four BM cell groups was performed, and the result showed that only ex vivo–induced BM-MDSCs presented inhibition of cell proliferation (Fig. 2E; BM-MDSC to T cell ratio: 1/1, $P < 0.001$; 1/2, $P < 0.01$). Furthermore, $Ly6G^{low}Ly6C^{hi}$ MO-MDSCs and $Ly6G^{hi}Ly6C^{low}$ PMN-MDSCs cocultured at a ratio of 1/1 and 1/5 were compared. Result showed only MO-MDSCs could decrease the ^{3}H-thymidine uptake (Fig. 2F; Mo-MDSC to T cell ratio: 1/1, $P < 0.001$; 1/5, $P < 0.01$). Last, the presence of an iNOS inhibitor led to the reversion of T cell proliferation (Fig. 2G; 1/2, $P < 0.001$; 1/5, $P < 0.001$) in the ex vivo–induced BM-MDSC/T cell cocultures. No suppressive effect was found in the assessment of PMN-MDSC/T cell co-cultures at different ratios (Supplementary Fig. S3).

To observe the effects of ex vivo–induced BM-MDSCs on the proliferation of $CD4^+$ and $CD8^+$ T cells in vitro, $CD3^+$ stimulation was introduced to enhance the proliferation of these T cell subsets. Overall, the presence of ex vivo–induced BM-MDSCs prevented the expansion of both $CD4^+$ and $CD8^+$ T cells. Fewer $CFSE^{low}$ cells were observed following co-culture with ex vivo–induced BM-MDSCs in a frequency-dependent manner (Figs. 3A and 3B). Compared with the $CD3^+$-stimulated group, the frequency of $CFSE^{low}$ cells decreased significantly in the presence of ex vivo–induced BM-MDSCs (Figs. 3C and 3D) in cocultures with a BM-MDSC ratio of 3/4 and 1/2 ($P < 0.001$ for both $CD4^+$ and $CD8^+$ T cells), whereas naive BM cells did not present such suppression of $CD4^+$ and $CD8^+$ T cells at both ratios ($P < 0.001$ and $P > 0.999$ for $CD4^+$ cell, and both $P > 0.999$ for $CD8^+$ T cells). Moreover, the addition of an iNOS inhibitor significantly ($P < 0.001$) reversed the effect of ex vivo–induced BM-MDSCs, whereas an ARG1 inhibitor had no obvious effects ($P > 0.9999$) on this process for both $CD4^+$ and $CD8^+$ T cells (Figs. 3E and 3F).

T Cell–Derived Cytokine Production is Modulated by Ex Vivo–Induced BM-MDSCs

Analysis of cytokines present in the supernatants of the T cell and ex vivo–induced BM-MDSC cultures showed that IFN-γ release increased significantly with allogeneic stimulation (6270.0 ± 299.2 pg/mL), whereas it was inhibited in the presence of ex vivo–induced BM-MDSCs (Fig. 4A; BM-MDSC ratios: 1/5, 2304.0 ± 287.3 pg/mL; 1/1, 1936.0 ± 84.67 pg/mL, $P < 0.001$). Naive BM cells did not show suppression of IFN-γ release ($P = 0.682$ and $P = 0.430$). In contrast, the IL-2 release increased significantly upon co-culture with ex vivo–induced BM-MDSCs (Fig. 4B; BM-MDSC ratios: 1/5, 999.6 ± 4.2 pg/mL; 1/1, 1062.0 ± 5.3 pg/mL, $P < 0.001$).

Investigative Ophthalmology & Visual Science

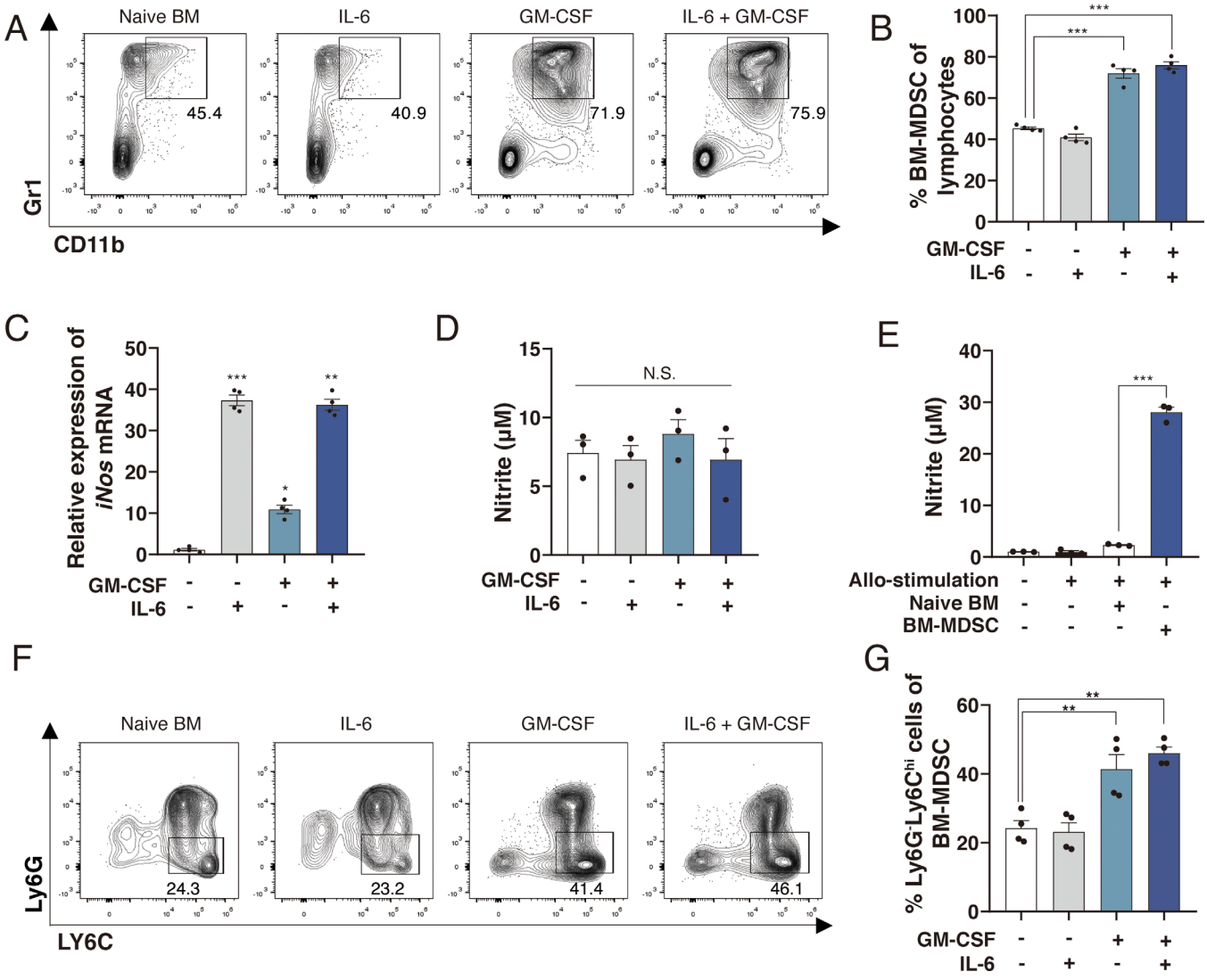

Figure 1. BM-MDSC and Ly6G^{low}Ly6C^{hi}MO-MDSC induction in vitro. **(A)** Representative flow cytometry data showing the frequency of CD11b^{+}Gr1^{+}BM-MDSCs induced with GM-CSF and IL-6 in vitro. **(B)** The frequency of BM-MDSCs increased significantly at day 4 with GM-CSF and IL-6 stimulus (n = 4; ***$P < 0.001$). **(C)** GM-CSF and IL-6-stimulated ex vivo–induced BM-MDSCs had higher *iNos* relative expression (n = 4, **$P < 0.01$, ***$P < 0.001$). **(D)** Nitrite levels among the different groups of incubated BM cells shows no significant difference (n = 3, $P = 0.64$). **(E)** Ex vivo–induced BM-MDSCs strongly promote nitrite release in allogeneic stimulation compared to naive BM cells (n = 3, ***$P < 0.001$). **(F)** Representative flow cytometry data showing the frequency of Ly6G^{low}Ly6C^{hi} MO-MDSCs. **(G)** The frequency of Ly6G^{low}Ly6C^{hi}MO-MDSCs increased significantly with GM-CSF and IL-6 stimulus (n = 4; **$P < 0.01$). Data are presented as the means ± SEM. BM-MDSC: bone marrow-derived myeloid-derived suppressor cells, GM-CSF: granulocyte macrophage-colony stimulating factor.

However, this effect was much less with naive BM cells (Fig. 4B; naïve-BM ratios: 1/5, 82.8 ± 0.4 pg/mL, $P < 0.001$; 1/1, 191.1 ± 2.0 pg/mL, $P < 0.001$). In the presence of 1/5 and 1/1 ex vivo–induced BM-MDSCs, IL-10 production was significantly increased (Fig. 4C; BM-MDSC ratios: 1/5, 361.3 ± 6.8 pg/mL; 1/1, 522.3 ± 8.5 pg/mL, $P < 0.001$). A similar increase was observed with naive BM cells (Fig. 4C; naïve-BM ratios: 1/5, 245.9 ± 1.1 pg/mL; 1/1, 344.5 ± 11.3 pg/mL; $P < 0.001$), although this increase was less than that with ex vivo–induced BM-MDSCs. TGF-β1 production with ex vivo–induced BM-MDSCs was significantly increased compared with allogeneic stimulation alone (Fig. 4D; BM-MDSC ratios: 1/5, 772.6 ± 10.4 pg/mL; 1/1, 935.7 ± 15.8 pg/mL, $P = 0.041$, $P < 0.001$, respectively). However, compared to the level of TGF-β1 in allogeneic stimulation (652.3 ± 46.4 pg/mL), there were no differences when co-culturing with naive BM cells (Fig. 4D; naive-BM ratios: 1/5, 652.8 ± 14.1 pg/mL; 1/1, 626.9 ± 14.4 pg/mL, both $P > 0.999$).

GM-CSF- and IL-6-Treated BM-MDSCs Promote Regulatory T Cell Expansion and Can Migrate Into Corneal Grafts

Treg frequency was assessed via flow cytometry on day 4 of T cell/ ex vivo–induced BM-MDSC co-culture under allogeneic stimulation, revealing increased numbers of Tregs (Fig. 5A). Compared with the naive T lymphocyte, naive BM cells and GM-CSF/IL-6-stimulated BM-MDSC groups, the frequency of CD4^{+}FOXP3^{hCD2+} cells was significantly higher in the presence of ex vivo-induced BM-MDSCs (Fig. 5B; $P < 0.001$). The migration of injected GFP^{+} ex vivo–induced

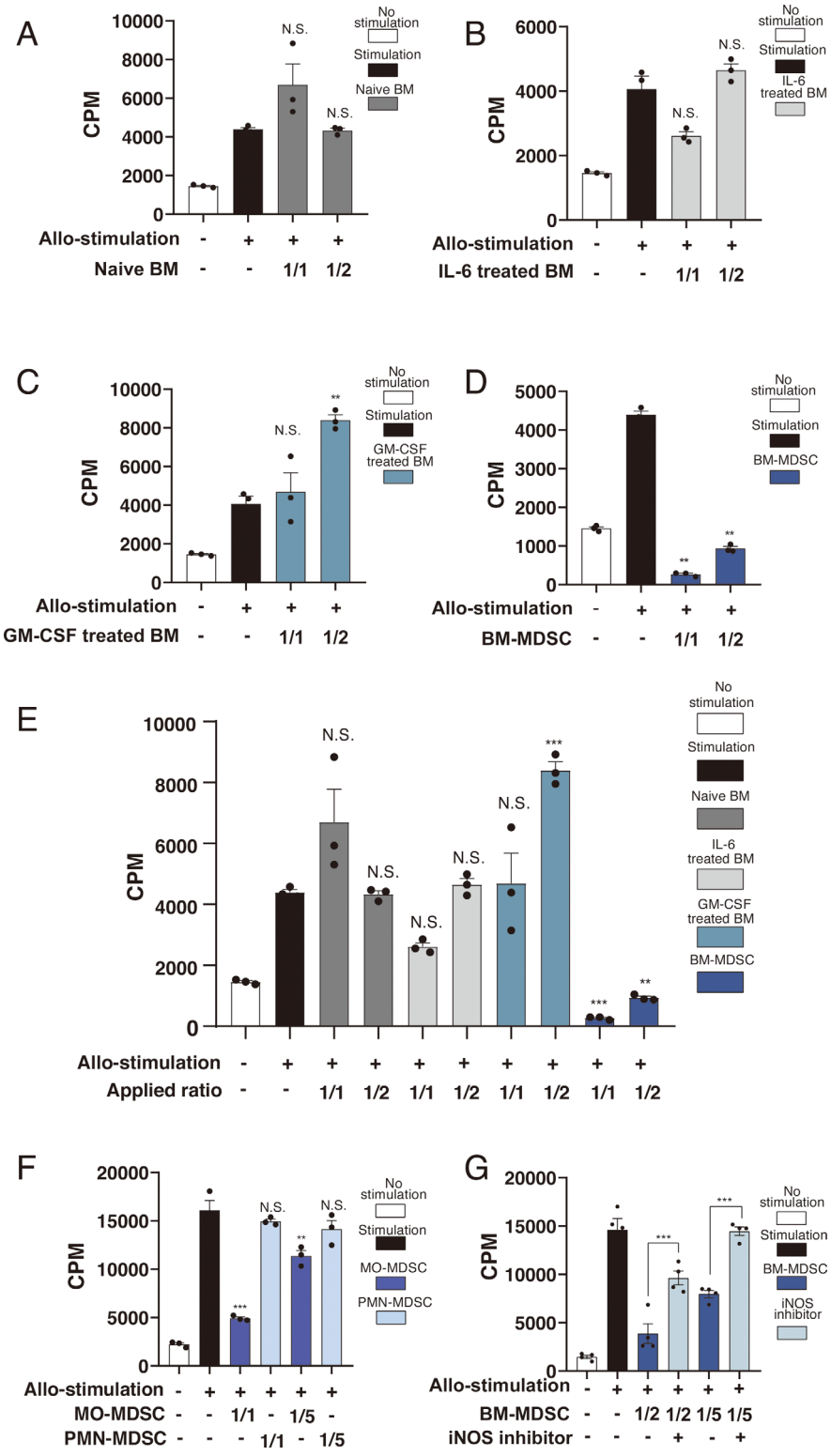

Figure 2. Ex vivo–induced BM-MDSCs suppress T lymphocyte proliferation via the iNOS pathway in the allogeneic stimulation of MLR assay. ^{3}H-thymidine uptake assay: **(A)** Bar graphs showing that naive BM cells increased the count per minute (CPM) in a dose-dependent manner (n = 3, naive BM cell ratio of 1/1, $P > 0.999$]; 1/2, $P = 0.109$). **(B)** IL-6-treated BM cells present no suppression of T lymphocyte proliferation either at ratio of 1/1 or 1/2 (n = 3, IL-6 treated BM cells ratio of 1/1, $P = 0.653$; 1/2, $P > 0.999$). **(C)** GM-CSF-treated BM cells shows no suppression (n = 3, 1/1, $P > 0.999$; 1/2, ($P = 0.003$). **(D)** Ex vivo–induced BM-MDSCs significantly reduced the CPM both at ratio of 1/1 and 1/2 (n = 3, GM-CSF-treated BM cell ratio of 1/1, $P = 0.005$; 1/2, $P = 0.007$]). **(E)** A comparison of the four treatments of BM cells used in MLR shows that only BM-MDSCs induced suppression (n = 3; $^{***}P < 0.001$, $^{**}P = 0.006$). **(F)** A comparison between Ly6G^{low}Ly6C^{hi} BM-MDSCs (monocytic-MDSCs, MO-MDSCs) and Ly6G^{hi}Ly6C^{low}BM-MDSCs (polymorphonuclear MDSCs, PMN-MDSCs) showed that the former presented suppression function of T lymphocyte proliferation, whereas the later did not. The suppression of MO-MDSCs was dose dependent (n = 3; $^{***}P < 0.001$, $^{**}P = 0.002$,). **(G)** The iNOS inhibitor inhibited the suppressive function of ex vivo–induced BM-MDSCs (n = 4, $^{***}P < 0.001$).

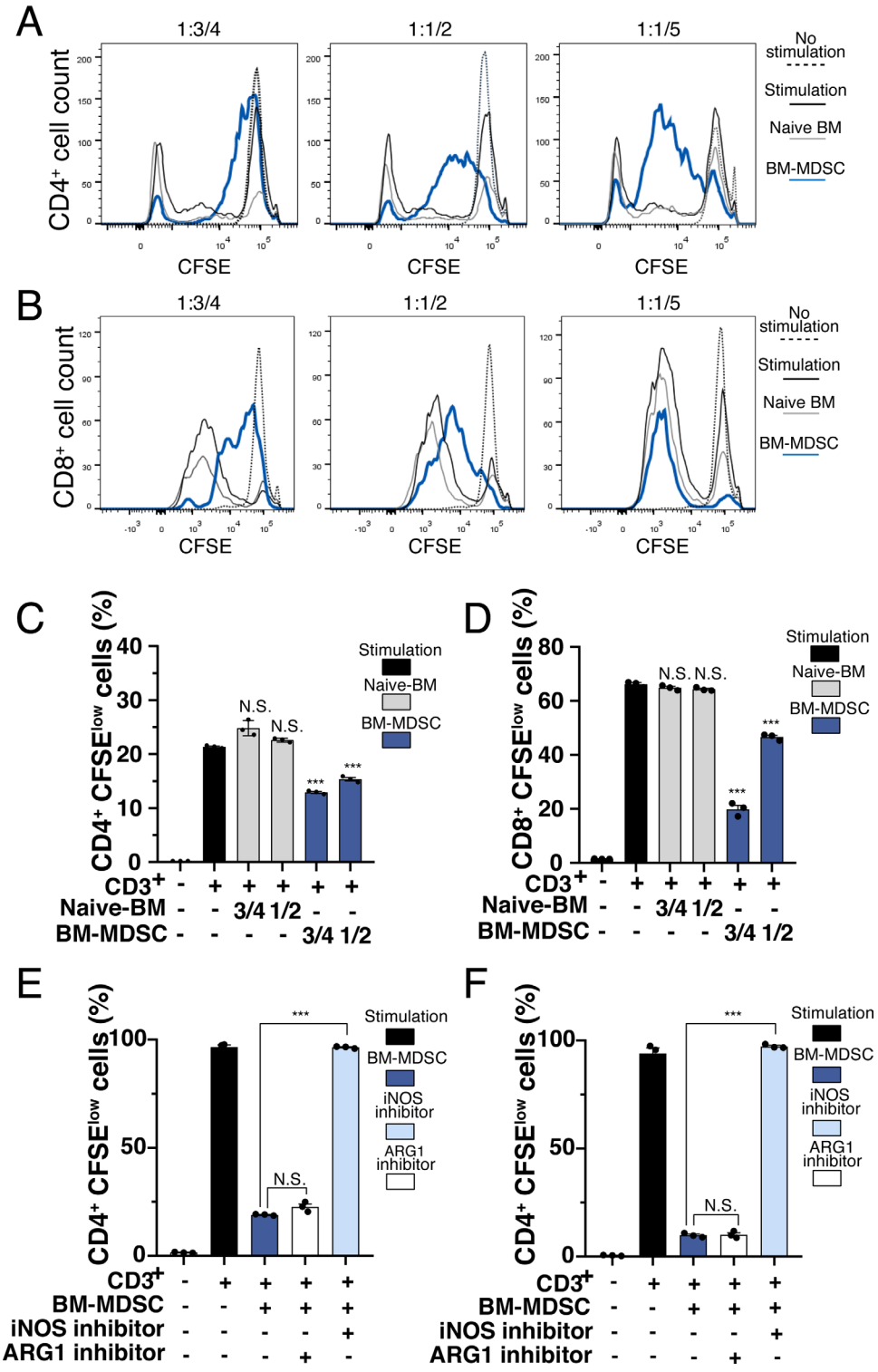

Figure 3. Ex vivo–induced BM-MDSCs inhibit $CD4^+$ and $CD8^+$ T cell proliferation. $CD4^+$ and $CD8^+$ T cells isolated from the cervical lymph nodes of BALB/C mice, labeled with CFSE, and cultured at 37°C. According to the progress of T cell proliferation, the frequencies of $CFSE^{low}$ cell distribution were observed using flow cytometry on day 3 to 4. The distribution of CFSE-labeled **(A)** $CD4^+$ and **(B)** $CD8^+$ T cells gradually drifted in the presence of different densities of ex vivo–induced BM-MDSCs (3/4, 1/2, and 1/5). The percentage of $CD4^+$ **(C)** and **(D)** $CD8^+$ T cells with low levels of CFSE labeling changed with different densities of ex vivo–induced BM-MDSCs present. Meanwhile, low levels of CFSE labeling $CD4^+$ and $CD8^+$ T cells with naive BM cells presented much higher frequency, which means lack of inhibition. Compared with simple $CD3^+$ stimulation, the iNOS inhibitor reversed the inhibition of $CD4^+$ **(E)** and $CD8^+$ T cells **(F)** by ex vivo–induced BM-MDSCs, whereas no such reversion was observed with the ARG1 inhibitor. ***$P < 0.001$, N.S. no significant difference. ARG, arginase-1.

Investigative Ophthalmology & Visual Science

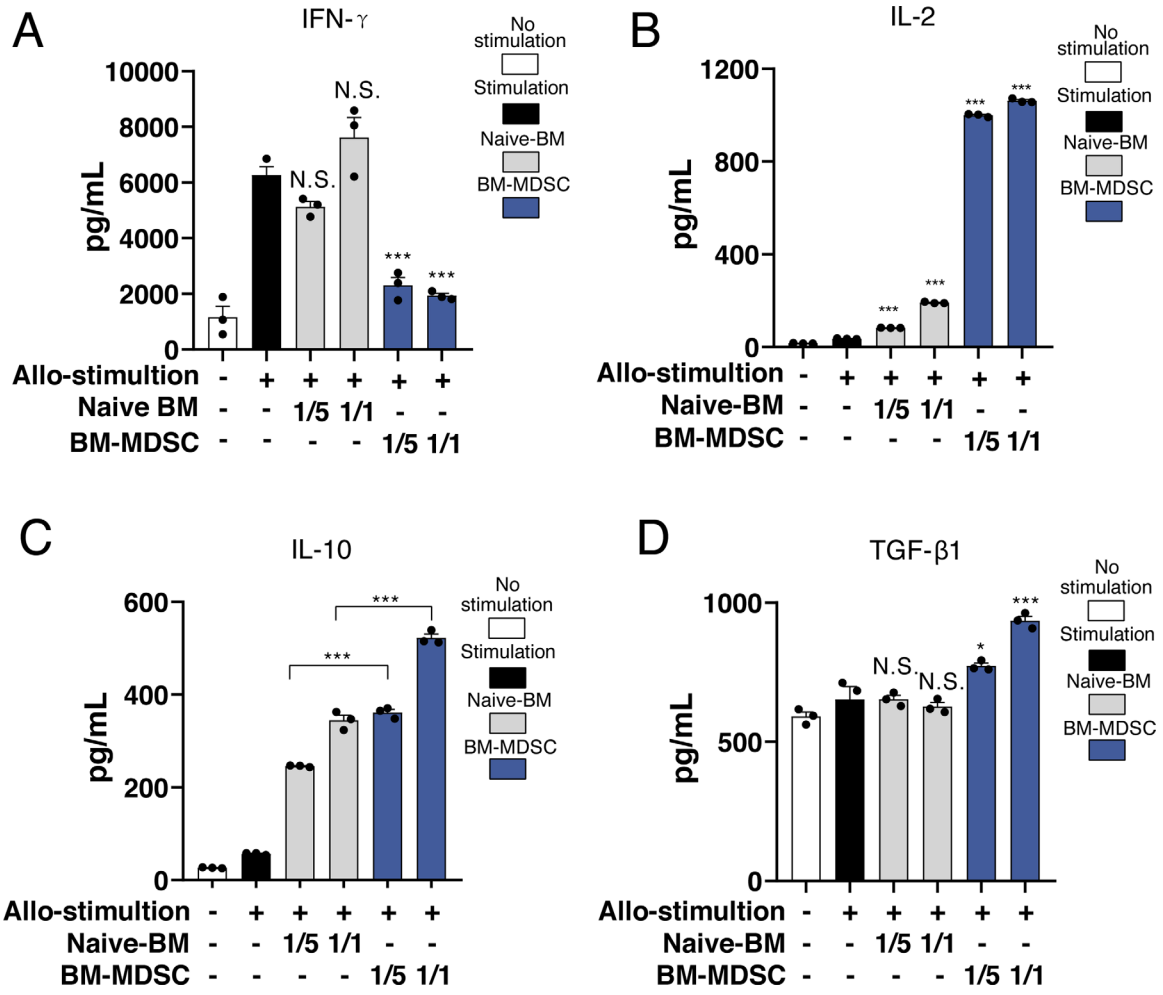

Figure 4. Ex vivo–induced BM-MDSCs reduce IFN-γ production and promote IL-2, IL-10, and TGF-β1 production in vitro. **(A)** Ex vivo–induced BM-MDSCs inhibited the production of IFN-γ in a dose-dependent manner (n = 3; ***$P < 0.001$). **(B)** The production of IL-2 (n = 3, ***$P < 0.001$), and **(C)** IL-10 (n = 3, ***$P < 0.001$) increased significantly when ex vivo–induced BM-MDSCs were present **(D).** TGF-β1 slightly increased when co-cultured with BM-MDSCs (n = 3, ***$P < 0.001$, *$P = 0.041$, N.S. $P > 0.999$).

BM-MDSCs after corneal transplantation was investigated using flow cytometry. GFP$^+$BM-MDSCs were found to migrate into the corneal grafts (Figs. 5C and 5D; $P < 0.001$).

Ex Vivo–Induced BM-MDSCs Reduce Immune Inflammatory Reactions and Prolong Corneal Graft Survival

Allogeneic high-risk corneal transplantation was performed to assess the impact of administering ex vivo–induced BM-MDSCs on graft survival, neovascularization, and lymphangiogenesis. Figures 6A to 6D shows the neovascularization, opacity, and survival of the grafts at eight weeks after BM-MDSC administration. Both the neovascularization and opacity scores increased to the maximum between days 21 and 28 after transplantation and reduced in the following weeks. At seven and eight weeks after transplantation, both the neovascularization (Fig. 6A; day 49, $P = 0.042$; day 56, $P = 0.042$) and opacity (Fig. 6B; day 42, $P = 0.008$; day 49, $P = 0.008$; day 56, $P < 0.001$) scores reduced significantly in grafts treated with the ex vivo–induced BM-MDSCs compared to untreated controls. Figure 6C shows the representative slit-lamp microscope photo at day 56 after corneal transplantation. At the end of the observation period, the corneal survival rates were significantly higher in the ex vivo–induced BM-MDSC-treated group (Fig. 6D; $P = 0.035$) than in other groups. Corneal graft immunohistochemistry revealed that the neovascularization and lymphatic vessel areas were reduced with ex vivo–induced BM-MDSC treatment (Fig. 6E), and the differences were significant for both CD31^{high}LYVE-1^{low} blood vessels (Fig. 6F; Control, 8.9 ± 0.3%; Naïve BM, 8.3 ± 0.7%; BM-MDSC, 6.1 ± 0.1, $P = 0.019$, compared to the control) and CD31^{low}LYVE-1^{high} lymphatic vessels (Fig. 6G; control, 5.8 ± 0.6%; naïve BM, 5.9 ± 0.8; BM-MDSC, 2.8 ± 0.5%, $P = 0.018$, compared to the control).

Discussion

Immune reaction control in the local environment is a key mechanism for prolonging corneal graft survival. Herein, the suppressive function of ex vivo–induced BM-MDSCs was investigated. Our results demonstrated that ex vivo–induced BM-MDSCs had immune suppressive functions via the iNOS pathway and expanded Tregs in vitro, indicating that ex vivo–induced BM-MDSCs could prolong corneal graft

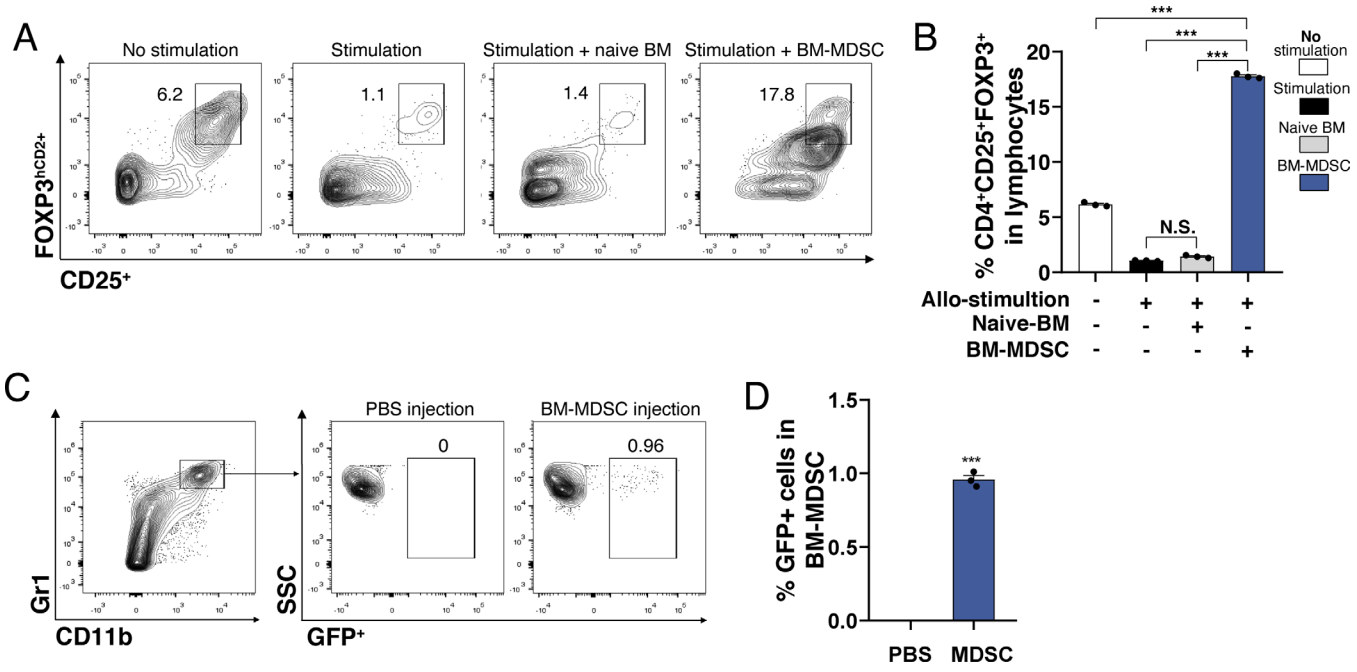

Figure 5. Ex vivo–induced BM-MDSCs promote $CD4^+FOXP3^{hCD2}$ cell expansion. **(A)** Representative flow cytometry data showing the increased frequency of $CD4^+Foxp3^{hCD2}$ cells (Tregs) upon co-culture with ex vivo–induced BM-MDSCs with allogeneic stimulation. **(B)** The frequency of Tregs among whole lymphocytes increased significantly with the ex vivo–induced BM-MDSC co-culture (n = 3, ***$P < 0.001$, N.S. $P = 0.104$). **(C)** $CD11b^+Gr1^+$BM-MDSCs tracked using GFP mouse cells presented in corneal grafts (n = 3, ***$P < 0.001$).

survival in an inflamed microenvironment, thus representing a potentially effective immunosuppressive therapy for corneal transplantation.

We found that IL-6 and GM-CSF co-cultures induced functional BM-MDSCs with iNOS upregulation. MDSCs were reportedly induced at a higher frequency with high GM-CSF levels in the tumor microenvironment,[28] and IL-6 reportedly stimulates MDSCs in multiple cancers.[29] However, these observations were made under tumor immunopathological conditions, mostly in the systemic environment, whereas the generation of MDSCs and their influence on the local corneal environment remain poorly understood. This study showed that BM-MDSCs expanded in the presence of GM-CSF, consistent with a previous study describing similar expansion and differentiation of MDSCs from umbilical cord blood with GM-CSF.[30] Interestingly, the relative mRNA expression of *iNos* increased significantly in the presence of both GM-CSF and IL-6. IL-6 could account for this increased expression. According to published studies,[31,32] IL-6 plays a role in inducing the expression of *iNos* as well as nitric oxide release in mouse. In our study, naive BM cells as well as coculture with IL-6 alone resulted in the death of most BM cells (more than 66%) in vitro. However, in combination with GM-CSF, a known cell growth factor,[33] the BM cells could survive and differentiate into sufficient BM-MDSCs. In many tumor microenvironments, *iNOS* is overexpressed and is known to be a tumor-mediated immunosuppression factor. It breaks down L-arginine and generates significant amounts of nitrite, which in turn prevents effector T cell activation through the Jak3/STAT5 signaling pathway that is critical for inflammatory and immune responses during the process of transplant rejection. Herein, it was demonstrated that the higher BM-MDSC number and their *iNos* expression were the result of combined GM-CSF and IL-6 signals. Thus ensuring a stable source of ex vivo–induced BM-MDSCs may benefit their application in corneal grafts.

The inhibition of T-cell proliferation by ex vivo–induced BM-MDSCs was shown to be reversed by an iNOS inhibitor, demonstrating that the suppression effect of BM-MDSCs is strongly related to the iNOS pathway. Previous studies showed that ARG1 expressed by MDSCs could also regulate T lymphocyte responses by impairing their proliferation and cytokine production.[34] However, in this study, no such effects were observed using an ARG1 inhibitor during the MLR assay. This agrees with the findings of Bian et al.,[35] who demonstrated that ARG1 is not required for the MDSC-mediated inhibition of T cell proliferation. Thus the iNOS pathway should be considered a major mechanism for the suppressive effect observed in the allogeneic immune microenvironment.

Furthermore, this study showed that ex vivo–induced BM-MDSCs suppressed T-cell proliferation between donor and recipient allogeneic lymphocyte reactions. As $CD4^+$ and $CD8^+$ cells are considered the major cells involved in graft rejection, their proliferation and relative cytokine production represent the state of the inflammatory environment, which is critical for graft outcome.[36] Our results showed that $CD8^+$ and $CD4^+$ T lymphocyte proliferation was inhibited in the presence of ex vivo–induced BM-MDSCs, concomitantly resulting in reduced IFN-γ secretion by these effector T cells. IFN-γ is a well-known proinflammatory cytokine associated with tissue damage; it was reported to be produced by alloreactive $CD8^+$ and $CD4^+$ T cells in mouse corneal graft rejection.[37,38] Therefore, by controlling effector T cell proliferation and their IFN-γ production, ex vivo–induced BM-MDSCs

Investigative Ophthalmology & Visual Science

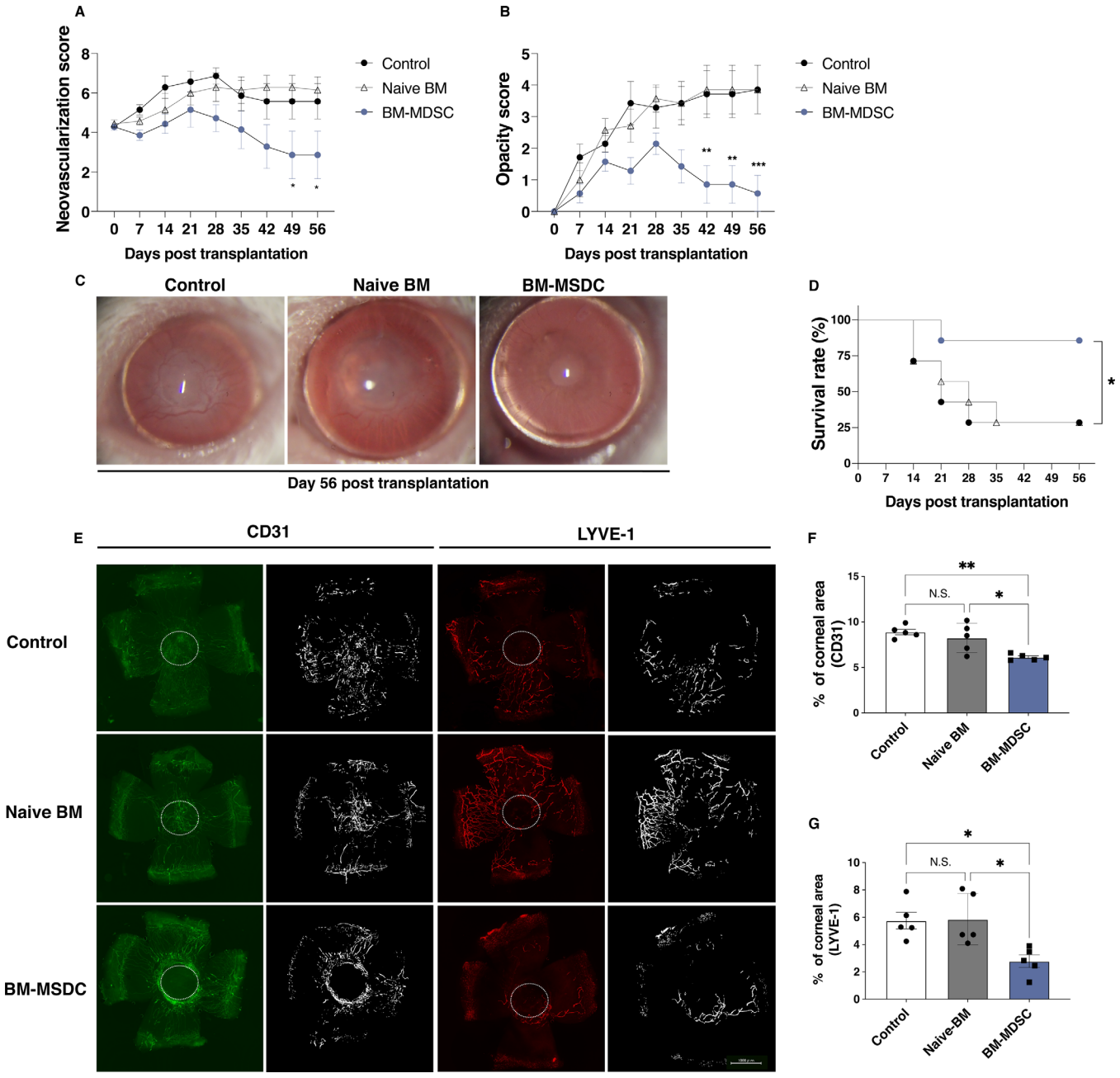

Figure 6. Ex vivo–induced BM-MDSC injection prolongs corneal graft survival and suppresses neovascularization. Neovascularization, opacity, and graft survival were assessed using a slit-lamp microscope. **(A)** The neovascularization score was markedly reduced in grafts with ex vivo–induced BM-MDSC injection compared to the control group (two-way ANOVA, n = 7/group; day 49, $^{*}P = 0.042$; day 56, $^{*}P = 0.042$). **(B)** Graft opacity scores reduced significantly in grafts with ex vivo–induced BM-MDSC injection compared to the control group (two-way ANOVA, n = 7/group; day 42, $^{**}P = 0.008$; day 49, $^{**}P = 0.008$; day 56, $^{***}P < 0.001$). **(C)** Representative slit-lamp microscope photos showing the grafted corneas at day 56 after corneal transplantation. **(D)** Kaplan-Meier survival curves show a significant increase in the survival of grafts with ex vivo–induced BM-MDSC injection compared to the control group (log-rank test, n = 7/group, $^{*}P = 0.035$). **(E)** Representative images showing CD31 (green) and LYVE-1 (red) staining in the corneal grafts. Graft areas show the white stiches. **(F)** The areas of $CD31^{high}LYVE\text{-}1^{low}$ blood vessels in corneal grafts injected with ex vivo-induced BM-MDSCs were significantly reduced compared to untreated controls (n = 5, $^{**}P = 0.003$, $^{*}P = 0.019$). **(G)** The areas of $CD31^{low}LYVE\text{-}1^{high}$ lymphatic vessels were significantly reduced in grafts administered ex vivo–induced BM-MDSCs compared to untreated controls (n = 5, $^{*}P = 0.023$, $^{*}P = 0.018$).

represent a reasonable method for creating a less inflammatory microenvironment.

Our results show the notable expansion of Tregs in the presence of ex vivo-induced BM-MDSCs. Tregs are immunosuppressors of the adaptive system, playing a critical role in modulating and maintaining immune tolerance. However, the amplification and induction of Tregs in an inflammatory environment were difficult owing to their plasticity.[39] It has been suggested that Tregs might become unstable under certain inflammatory conditions, and their phenotype could change. In tumor-bearing hosts, MDSCs reportedly mediate the development of Tregs and T cell anergy.[40] In

this study, we showed an increased Treg frequency with allogeneic stimulation via ex vivo–induced BM-MDSC intervention. This suggests that Treg expansion is applicable in an ex vivo inflammatory microenvironment. Considering the immunosuppressive function of Tregs, expanding their number via ex vivo–induced BM-MDSCs should be a feasible approach for regulating effector T cell responses. Shao et al.[25] reported that local delivery of Treg promotes corneal allograft survival. Combined with our discovery, it would be exciting to further investigate whether and how the BM-MDSC-induced expanded Tregs exert suppressive function in corneal grafts.

In the presence of ex vivo-induced BM-MDSCs in the inflammatory microenvironment, the production of immunosuppressive cytokines, such as IL-2, IL-10, and TGF-β1 increased. IL-10 and TGF-β are important in tolerance induction and immune regulation, and IL-2 is involved in the development of Tregs.[41] IL-2 mediates its effects by binding to an IL-2 receptor that is highly expressed on Tregs and activated T cells, subsequently promoting Treg expansion.[41,42] These increased immunosuppressive cytokines may promote Treg expansion and maintenance in the inflammatory microenvironment, which may help corneal graft survival in vivo.

Furthermore, this study showed that the ex vivo–induced BM-MDSC injection prevented local neovascularization and prolonged grafted cornea survival in vivo in high-risk corneal transplantation conditions. Typically, MDSCs are applied in in vivo models via local and intravenous injections; however, in our high-risk corneal graft models, we applied ex vivo–induced BM-MDSCs through sub-conjunctival injection, which may improve the odds of direct interaction. This study elucidated the migration of locally delivered ex vivo–induced BM-MDSCs and demonstrated their suppressive effects on the immune response against the allograft. To our knowledge, this is the first report to observe the effects of ex vivo–induced BM-MDSCs through injection into the nearest site to the grafts. During the process of rejection, lymphatic vessels and neovascular tissues are important factors that support the immune and inflammation response, as donor antigens, inflammatory cells, and pro-inflammatory cytokines could be delivered through these vessels to the graft. For corneal graft survival, reducing neovascularization and lymphangiogenesis is vital,[43,44] and such reduction was confirmed in our high-risk mouse corneal grafts.

Nevertheless, this study has some limitations. First, this study only presented the effectiveness of ex vivo–induced BM-MDSCs applied in mouse corneal allografts. We found decreased mRNA expression of inflammatory cytokines including IFN-γ, TGF-β1, IL-1β, and VEGF-A in the corneal grafts after BM-MDSC administration (Supplementary Fig. S4); however, the mechanisms mediated in this allogeneic corneal graft model are complicated and remain unsolved. Second, only entire populations of BM-MDSCs and T cells were investigated, excluding other cell types, such as specific subsets of BM-MDSCs, natural killer cells, and plasmacytoid dendritic cells, which also independently contribute to the overall immune response network in corneal graft rejection. Third, the manner in which BM-MDSCs and Tregs migrated within the grafts, and whether their suppressive function is antigen-specific, should be determined in future studies.

Our results indicate that ex vivo–induced BM-MDSCs could prolong the survival of high-risk corneal grafts. The inhibitory effects of ex vivo–induced BM-MDSCs on T cell proliferation and Treg expansion represent the basic in vitro mechanism, suggesting that ex vivo–induced BM-MDSCs could represent a promising approach for improving corneal graft rejection in vivo.

Acknowledgments

The authors thank Dan Gao, for her helpful insights during scientific discussions.

Supported by JSPS KAKENHI Grant Numbers 16K20332 (TI), 18K16935 (TI), 20K09810 (TI), and 20K22985 (KF). Jun Zhu was the recipient of a fellowship provided by the Japan-China Sasakawa Medical Fellowship program (grant number 2018314).

Disclosure: **J. Zhu,** None; **T. Inomata,** None; **K. Fujimoto,** None; **K. Uchida,** None; **K. Fujio,** None; **K. Nagino,** None; **M. Miura,** None; **N. Negishi,** None; **Y. Okumura,** None; **Y. Akasaki,** None; **K. Hirosawa,** None; **M. Kuwahara,** None; **A. Eguchi,** None; **H. Shokirova,** None; **A. Yanagawa,** None; **A. Midorikawa-Inomata,** None; **A. Murakami,** None

References

1. Gain P, Jullienne R, He Z, et al. Global survey of corneal transplantation and eye banking. *JAMA Ophthalmol*. 2016;134:167–173.
2. Mathews PM, Lindsley K, Aldave AJ, Akpek EK. Etiology of global corneal blindness and current practices of corneal transplantation: a focused review. *Cornea*. 2018;37:1198–1203.
3. Dana MR, Qian Y, Hamrah P. Twenty-five-year panorama of corneal immunology: emerging concepts in the immunopathogenesis of microbial keratitis, peripheral ulcerative keratitis, and corneal transplant rejection. *Cornea*. 2000;19:625–643.
4. Inomata T, Hua J, Nakao T, et al. Corneal tissue from dry eye donors leads to enhanced graft rejection. *Cornea*. 2018;37:95–101.
5. Inomata T, Mashaghi A, Di Zazzo A, Lee SM, Chiang H, Dana R. Kinetics of angiogenic responses in corneal transplantation. *Cornea*. 2017;36:491–496.
6. Niederkorn JY. High-risk corneal allografts and why they lose their immune privilege. *Curr Opin Allergy Clin Immunol*. 2010;10:493–497.
7. Sakaguchi S, Sakaguchi N. Regulatory T cells in immunologic self-tolerance and autoimmune disease. *Int. Rev. Immunol.*. 2005;24:211–226.
8. Inomata T. A new immunotherapy using regulatory T-cells for high-risk corneal transplantation. *JMJ*. 2017;63:2–7.
9. Ono M. Control of regulatory T-cell differentiation and function by T-cell receptor signaling and Foxp3 transcription factor complexes. *Immunology*. 2020;160:24–37.
10. Inomata T, Hua J, Di Zazzo A, Dana R. Impaired function of peripherally induced regulatory T cells in hosts at high risk of graft rejection. *Sci Rep*. 2016;6:39924.
11. Hua J, Inomata T, Chen Y, et al. Pathological conversion of regulatory T cells is associated with loss of allotolerance. *Sci Rep*. 2018;8:7059.
12. Iizuka-Koga M, Nakatsukasa H, Ito M, Akanuma T, Lu Q, Yoshimura A. Induction and maintenance of regulatory T cells by transcription factors and epigenetic modifications. *J Autoimmun*. 2017;83:113–121.
13. Palucka K, Banchereau J. Dendritic-cell-based therapeutic cancer vaccines. *Immunity*. 2013;39:38–48.

14. Verhagen J, Wegner A, Wraith DC. Extra-thymically induced T regulatory cell subsets: the optimal target for antigen-specific immunotherapy. *Immunology*. 2015;145:171–181.
15. Vandermeulen M, Erpicum P, Weekers L, et al. Mesenchymal stromal cells in solid organ transplantation. *Transplantation*. 2020;104:923–936.
16. Yang L, DeBusk LM, Fukuda K, et al. Expansion of myeloid immune suppressor Gr+CD11b+ cells in tumor-bearing host directly promotes tumor angiogenesis. *Cancer Cell*. 2004;6:409–421.
17. Fujimura T, Mahnke K, Enk AH. Myeloid derived suppressor cells and their role in tolerance induction in cancer. *J Dermatol Sci*. 2010;59:1–6.
18. Liechtenstein T, Perez-Janices N, Gato M, et al. A highly efficient tumor-infiltrating MDSC differentiation system for discovery of anti-neoplastic targets, which circumvents the need for tumor establishment in mice. *Oncotarget*. 2014;5:7843–7857.
19. Ren Y, Dong X, Zhao H, et al. Myeloid-derived suppressor cells improve corneal graft survival through suppressing angiogenesis and lymphangiogenesis. *Am J Transplant*. 2021;21:552–566.
20. Liu X, Quan N. Immune cell isolation from mouse femur bone marrow. *Bio Protoc*. 2015;5:e1631.
21. Tanaka Y, Ohdan H, Onoe T, Asahara T. Multiparameter flow cytometric approach for simultaneous evaluation of proliferation and cytokine-secreting activity in T cells responding to allo-stimulation. *Immunol Invest*. 2004;33:309–324.
22. Ogawa M, Inomata T, Shiang T, Tsubota K, Murakami A. Method for selective quantification of immune and inflammatory cells in the cornea using flow cytometry. *J Biol Methods*. 2018;5:e102.
23. Inomata T, Mashaghi A, Di Zazzo A R. D. Ocular surgical models for immune and angiogenic responses. *J Biol Methods*. 2015;2(3):e27.
24. Hua J, Stevenson W, Dohlman TH, et al. Graft site microenvironment determines dendritic cell trafficking through the CCR7-CCL19/21 axis. *Invest Ophthalmol Vis Sci*. 2016;57:1457–1467.
25. Shao C, Chen Y, Nakao T, et al. Local delivery of regulatory T cells promotes corneal allograft survival. *Transplantation*. 2019;103:182–190.
26. Choi W, Ji YW, Ham HY, et al. Gr-1intCD11b+ myeloid-derived suppressor cells accumulate in corneal allograft and improve corneal allograft survival. *J Leukoc Biol*. 2016;100:1453–1463.
27. Gabrilovich DI. Myeloid-derived suppressor cells. *Cancer Immunol Res*. 2017;5:3–8.
28. Marigo I, Dolcetti L, Serafini P, Zanovello P, Bronte V. Tumor-induced tolerance and immune suppression by myeloid derived suppressor cells. *Immunol Rev*. 2008;222:162–179.
29. Jiang M, Chen J, Zhang W, et al. Interleukin-6 trans-signaling pathway promotes immunosuppressive myeloid-derived suppressor cells via suppression of suppressor of cytokine signaling 3 in breast cancer. *Front Immunol*. 2017;8:1840.
30. Park MY, Lim BG, Kim SY, Sohn HJ, Kim S, Kim TG. GM-CSF promotes the expansion and differentiation of cord blood myeloid-derived suppressor cells, which attenuate xenogeneic graft-vs.-host disease. *Front Immunol*. 2019;10:183.
31. Kang KW, Wagley Y, Kim HW, et al. Novel role of IL-6/SIL-6R signaling in the expression of inducible nitric oxide synthase (iNOS) in murine B16, metastatic melanoma clone F10.9, cells. *Free Radic Biol Med*. 2007;42:215–227.
32. da Silva Krause M, Bittencourt A, Homem de Bittencourt PI, Jr., et al. Physiological concentrations of interleukin-6 directly promote insulin secretion, signal transduction, nitric oxide release, and redox status in a clonal pancreatic beta-cell line and mouse islets. *J Endocrinol*. 2012;214:301–311.
33. Becher B, Tugues S, Greter M.GM-CSF: from growth factor to central mediator of tissue inflammation. *Immunity*. 2016;45:963–973.
34. Zea AH, Rodriguez PC, Atkins MB, et al. Arginase-producing myeloid suppressor cells in renal cell carcinoma patients: a mechanism of tumor evasion. *Cancer Res*. 2005;65:3044–3048.
35. Bian Z, Abdelaal AM, Shi L, et al. Arginase-1 is neither constitutively expressed in nor required for myeloid-derived suppressor cell-mediated inhibition of T-cell proliferation. *Eur J Immunol*. 2018;48:1046–1058.
36. Inomata T, Fujimoto K, Okumura Y, et al. Novel immunotherapeutic effects of topically administered ripasudil (K-115) on corneal allograft survival. *Sci Rep*. 2020;10:19817.
37. Hegde S, Beauregard C, Mayhew E, Niederkorn JY. CD4(+) T-cell-mediated mechanisms of corneal allograft rejection: role of Fas-induced apoptosis. *Transplantation*. 2005;79:23–31.
38. Braun MY, Desalle F, Le Moine A, et al. IL-5 and eosinophils mediate the rejection of fully histoincompatible vascularized cardiac allografts: regulatory role of alloreactive CD8(+) T lymphocytes and IFN-gamma. *Eur J Immunol*. 2000;30:1290–1296.
39. Sakaguchi S, Vignali DA, Rudensky AY, Niec RE, Waldmann H. The plasticity and stability of regulatory T cells. *Nat Rev Immunol*. 2013;13:461–467.
40. Huang B, Pan PY, Li Q, et al. Gr-1+CD115+ immature myeloid suppressor cells mediate the development of tumor-induced T regulatory cells and T-cell anergy in tumor-bearing host. *Cancer Res*. 2006;66:1123–1131.
41. Tahvildari M, Inomata T, Amouzegar A, Dana R. Regulatory T cell modulation of cytokine and cellular networks in corneal graft rejection. *Curr Ophthalmol Rep*. 2018;6:266–274.
42. Tahvildari M, Omoto M, Chen Y, et al. In vivo expansion of regulatory T cells by low-dose interleukin-2 treatment increases allograft survival in corneal transplantation. *Transplantation*. 2016;100:525–532.
43. Dana MR. Angiogenesis and lymphangiogenesis-implications for corneal immunity. *Semin Ophthalmol*. 2006;21:19–22.
44. Di Zazzo A, Lee S-M, Sung J, et al. Variable responses to corneal grafts: insights from immunology and systems biology. *J. Clin. Med*. 2020;9:586.

Investigative Ophthalmology & Visual Science